Article:

Collins, R. and Boxall, J. (2012) The Influence of Ground Conditions on Intrusion Flows through Apertures in Distribution Pipes. Journal of Hydraulic Engineering, 139 (10). 1052 - 1061. ISSN 0733-9429

https://doi.org/10.1061/(ASCE)HY.1943-7900.0000719

The Influence of Ground Conditions on Intrusion Flows through Apertures in Distribution Pipes

Richard Collins [1] and Joby Boxall [2]

ABSTRACT

This paper presents a new, tractable analytical expression to describe the intrusion of fluids into buried pipes under steady-state conditions. The expression is validated with results from novel experiments. The derivation is based on the combination of the relevant existing models of flows through porous media and the losses through an orifice, with the resulting expression relating the intrusion flow rate to an applied driving pressure. The expression is shown to yield results directly equivalent to those generated from a full 3D CFD model of the intrusion process. Results from the experiments, quantifying volumetric intrusion from a realistic 3D porous media, presented here, compare favourably with calculated values, validating the expression. While the experimental and analytical results show a high level of agreement, it was found that the analytical expression tends to slightly under estimate the intrusion rate seen experimentally. The absolute difference in the values is low and is thought to be attributed to preferential flow path at the porous media and pipe interface that the analytical expression and CFD model do not include. It is shown mathematically and verified experimentally that the viscous and inertial resistance to flow in the porous media reduces the intrusion (or leakage) flow over that predicted by the standard orifice equation and places additional dependencies of the flow on the size of the intrusion orifice. The values obtained from the expression should be considered as a lower bound to intrusion (and leakage) rates, with upper bounds being provided by the standard orifice equation. Although developed to aid in the quantification of intrusion risk, such as associated with water distribution systems, the expression

[1]Department of Civil and Structural Engineering, University of Sheffield, Mappin Street, Sheffield, S1 3JD, UK, email: r.p.collins@shef.ac.uk

[2]Department of Civil and Structural Engineering, University of Sheffield, Mappin Street, Sheffield, S1 3JD, UK, email: j.b.boxall@shef.ac.uk

is also validated for leakage for the limited case that the external porous media is considered to be fully compacted, consolidated and immobile.

INTRODUCTION

Pressurised pipes transport large volumes of some of the worlds most precious and/or vital resources; whether that be oil and gas or drinking water. It is therefore vitally import to ensure that these resources are not lost through leakage or contaminated by intrusion of unwanted physical biological or chemical agents. Contaminant intrusion is particularly important in ageing Water Distribution Systems (WDS) where there is concern that leakage points and cross connections provide a potential pathway into the system. Once in the WDS the contaminants would then be transported to customers and hence pose a risk to human health.

Lindley and Buchberger (2002) laid out three requirements for there to be a risk to human health due to intrusion; there needs to be a pathway (leak, badly fitted joint, air valve, cross connection), a driving force (pressure gradient) and the existence of a contaminant immediately external to the pipe. The existence of leaks and hence pathways in WDS are well known. Due to the dynamic nature of distribution systems, transient pressure waves and longer term de-pressurisation events are known to occur (Walski and Lutes 1994; Kirmeyer et al. 2001; Gullick et al. 2004; Friedman et al. 2004; Fleming et al. 2007; Besner et al. 2007) and could provide the required driving force. These studies have reported low or negative pressure events occurring for varying durations, from fractions of seconds to a number of minutes. There have also been a number of studies on the existence of pathogens and chemicals in the environment surrounding water pipes (LeChevallier et al. 2003; Karim et al. 2003; Besner et al. 2007). It therefore appears that the three theoretical requirements for intrusion are fulfilled and there have also been a number of the cases where intrusion has been the primary suspect in water quality failures (Kirmeyer et al. 2001; Friedman et al. 2004), however the existence of contamination events in water distribution systems is yet to be categorically confirmed.

To begin to be able to quantify the risk of intrusion to human health it is proposed that it is not sufficient to simply acknowledge the existence of the three requirements determined by Lindley and Buchberger. In particular it is important to understand how the low or negative pressures interact with the pathway, the surrounding soil and the contaminant to produce the intrusion event, and how they determine the magnitude of the possible intrusion event. In previous studies this interaction has simply been modelled using the standard orifice equation (Kirmeyer et al. 2001; Karim et al. 2003; Besner et al. 2007)

$$Q = C_d \frac{\pi d_o^2}{4} \sqrt{2g\Delta h} \tag{1}$$

where Q is the volumetric intrusion flow rate, C_d is a coefficient of discharge of the orifice, d_0 the orifice diameter and Δh the difference in the static head between the pipe and the head of ground water external to the pipe. Based on this model intrusion will therefore occur the moment that the static head inside the pipe drops below the external head and is always proportional to the square root of that pressure difference. The orifice equation, although benefiting from simplicity, does not take into account the effects of the surrounding soil conditions, the effect of pressure changes on the orifice diameter, the transient nature of the flow through the orifice, the coupling of the intrusion flow and the driving pressure and the re-intrusion of water that originated in the pipe.

To improve understanding of the intrusion process an analytical expression of the flow into a pipe orifice buried in a homogeneous isotropic saturated porous media is presented here. The model developed provides a more realistic account of intrusion than the orifice equation at no great increase in complexity and using known or parameters that it is possible to estimate. Experimental results validating the technical expression are presented.

BACKGROUND

A preliminary experimental study into transient driven hydraulic exchange required for intrusion into water distribution systems was undertaken by Boyd et al. (2004a, 2004b). Transients were generated by either upstream valve closures or pump trips, with an intrusion element of a column of water directly attached to the pipe. The paper confirmed intrusion occurred, however was inconclusive in assessing severity or the relative significance of contributing factors.

Lopez-Jimenez et al. (2010) developed a 3D steady-state Computational Fluid Dynamics (CFD) intrusion model for the case of a small scale pipe with a circular orifice surrounded by water only, comparing it to experimental results with a good level of agreement. Collins *et al.* (2010) also modelled steady state intrusion into a pipe system using 3D CFD but considering both intrusion from water only and porous media surrounding the pipe. The porous media was modelled as saturated with both viscous and inertial resistance. In the case of the porous media the steady-state intrusion rates were reduced with respect to the water only case, but remained proportional to the square root of the driving pressure. The porous media modified the coefficient of discharge and added dependencies on the properties of the media and interestingly adds further dependencies on the size of the orifice. The results showed a highly 3D external flow field with rapid dissipation of pressure and flow rate with distance.

Walski *et al.* (2006) proposed a model of leakage from a pipe that accounts for the loss in a soil by assuming the flow from an orifice is piped vertically to the surface of a saturated porous media. The model couples the head loss due to the orifice and the head loss through the soil:

$$\Delta h = h_o + h_s \tag{2}$$

where h_o is the head loss through the orifice and h_s the head loss through the soil. The head loss through the orifice is modelled using the orifice equation (1), and the loss through the soil using the Darcy equation for seepage flows in porous media. The proposed model appears to match well with experimental data. However it is known that the Darcy equation is only valid for Reynolds numbers below 10, where the characteristic length of the Reynolds number is the mean particle diameter. This would have been invalid in many of the experimental cases, indeed Walski (2006) noted that in some cases the fluid velocity was at the point of fluidisation. Typically the orifice size was an order of magnitude smaller in diameter than the column of porous media. There would have been a significant decrease in pressure due to this expansion. Further issues with soil mechanics where highlighted in a paper by Cassa and van Zyl (2011), in which they describe the mounding, soil fracture and void formation that would have an effect on leakage and by extension intrusion rates. Similar tests were presented in Collins *et al.* (2011) which describes the intrusion of water due to transient low pressures through various types of orifice and porous media, when the porous media is constrained in a vertical measuring cylinder. Results in the article show that the properties of the porous media, as well as the size of the orifice have a significant impact on the total intruded volume for a given transient.

DERIVATION OF NEW ANALYTICAL EXPRESSION FOR INTRUSION FLOW RATES

Equations for intrusion flow rates into a circular orifice in a pipe buried to a depth, D, under the free surface of a saturated soil are developed. In order to facilitate a tractable solution the soil is assumed to by homogeneous and isotropic with the flow to the orifice being radial, and spherically symmetrical in all directions, while this is an idealisation the CFD work of Collins *et al.* (2010) supports this approach. Using a similar conceptual approach to Walski *et al.* (2006), it follows that the difference in the head in the pipe and the hydrostatic head due to the burial depth of the pipe below the saturated free surface must be accounted for by the head loss in the soil and the head loss through the orifice.

$$\Delta h = h_p - D = h_o + h_s \tag{3}$$

where h_p is the pressure head in the pipe, and D is the burial depth beneath the saturated surface.

Head Loss through Porous Media

Flow through a fully saturated porous media has been extensively studied in a number of fields, from hydrology, mining engineering to chemical and process engineering. The widely known Darcy equation (Bear 1988) gives the pressure drop along streamlines in the media for slowly flowing fluids:

$$\frac{dh_s(s)}{ds} = A \cdot q(s) \tag{4}$$

where s is the arclength along the streamline, $h(s)$ is the piezometric head, $q(s)$ the specific flow rate through the porous media (it should be noted that this is the total volumetric flow rate divided by the area of flow and not the actual velocity of a packet of fluid in the porous media), and

A the viscous resistance of the porous media. A is related to the more commonly referenced hydraulic conductivity, K, by $A = \frac{1}{K}$. The Darcy equation is known to be valid for Reynolds numbers below 10, where the characteristic length of the Reynolds number is the mean particle diameter, at higher Reynolds numbers a significant non-linearity is seen. This non-linearity will incur significantly increased pressure loss in the soil over that predicted by the Darcy relationship. In 1901 Forchhiemer (1901) proposed an equation with an additional term, proportional to the direction preserving square of the specific flow rate, to account for this non-linearity:

$$\frac{dh_s(s)}{ds} = A \cdot q(s) + B \cdot |q(s)|\, q(s) \tag{5}$$

where B is the inertial resistance of the porous media. The direction preserving square term can be simplified to a simple square term if the sign of $q(s)$ remains constant and care is taken to define the direction of positive flow rate.

Ergun Equation

Relationships to determine the values of A and B in (4) and (5) for porous media composed of packed granular particles have been developed by Ergun (1952) based on the mean particle diameter, porosity and the viscosity of the penetrating fluid:

$$\begin{aligned} A &= \frac{150\,\mu}{\psi_p^2\, d_p^2\, \rho\, g} \frac{(1-\epsilon)^2}{\epsilon^3} \\ B &= \frac{1.75}{\psi_p\, d_p\, g} \frac{(1-\epsilon)}{\epsilon^3} \end{aligned} \tag{6}$$

with d_p the mean particle diameter, ψ_p the particle shape factor (equal to 1 for spherical particles), ϵ the porosity of the media, ρ and μ the fluid density and dynamic viscosity and g the acceleration due to gravity. Similar relationships have also been found by Barr (2001) based on the particle surface area.

Equation (5) provides a description of the motion of the fluid in the porous media; a conservation equation is also required to calculate the intrusion flow rates. From Bear (1988) the volume conservation equation for the steady state flow of an incompressible fluid through a homogeneous and isotropic porous media is given as:

$$\nabla \cdot \mathbf{q} = 0 \tag{7}$$

thus the flow in porous media is seen to be a diffusion relationship.

Geometry of the Intrusion into Orifices

It was shown in Collins *et al.* (2010) using CFD modelling that intruding flow will enter an orifice from all directions, see Figure 1a), with the flow paths being diverted as they flow past the pipeline. If the diameter of the pipe is small compared to the size of the region of flow then this flow field will increasing appear to be a point sink in a three dimensional flow field Figure 1b). Hence in this work the external flow field is modelled as spherically symmetrical with the intrusion orifice as a sink at the center. The external boundary of the flow field is at D the pipe burial depth below the saturated surface. The sink of the flow field is at radius R, a radius that will be determined to ensure that the flow velocities and head losses are accurately represented, being similar to those exiting the orifice.

By assuming purely radial steady-state intrusion towards the center sink, Equation (7) becomes:

$$\frac{d}{dr}(r^2 q(r)) = 0 \tag{8}$$

where the arclength of the flow lines is replaced by the radial distance from the center of the sphere. It is then trivial to integrate (8) to give the specific flow rate as a function of the radial distance from the center:

$$q(r) = \frac{C}{r^2} \tag{9}$$

with C as the constant of integration. The constant of integration can be found by considering the total volumetric flow rate through the soil. The total volumetric flow, Q_s, is found by multiplying the specific flow rate by the area of a sphere that the flow rate passes through, $Q_s = 4\pi r^2 \cdot q(r)$, therefore:

$$
\begin{aligned}
q(r) =& \frac{C}{r^2} = \frac{Q_s}{4\pi r^2} \\
C =& \frac{Q_s}{4\pi}
\end{aligned}
\tag{10}
$$

If the discharge is constrained to only expand into a fraction of the sphere due to the local geometry, such as the pipe wall or other boundary, a geometry factor G needs to be included:

$$
q(r) = G\frac{C}{r^2} \tag{11}
$$

It is thought that the geometric term will be some combination of the pipe diameter and orifice size. The constant of integration C is not affected by the inclusion of the geometric term as the total flow rate from the soil is unaffected.

Equation (10) can the be substituted into (11) for specific flow rates which can then be combined with the momentum equation (5) to give the head loss per unit radius in the soil:

$$
\frac{dh_s(r)}{dr} = \frac{1}{4}\frac{A\,G\,Q_s}{\pi\,r^2} + \frac{1}{16}\frac{B\,G^2\,Q_s^2}{\pi^2\,r^4} \tag{12}
$$

The total head loss Equation (12) can be integrated over the soil domain to give the total head loss through the soil:

$$
h_s = \int_R^D \frac{dh(r)}{dr}dr = \left(\frac{1}{R} - \frac{1}{D}\right)\frac{A\,G\,Q_s}{4\pi} + \left(\frac{1}{R^3} - \frac{1}{D^3}\right)\frac{B\,G^2\,Q_s^2}{48\pi^2} \tag{13}
$$

If it is assumed that the burial depth of the pipe below the saturated surface of the soil is significantly larger than the radius of the internal boundary, $D \gg R$, then:

$$
\begin{aligned}
\frac{1}{R} - \frac{1}{D} \approx \frac{1}{R} \\
\frac{1}{R^3} - \frac{1}{D^3} \approx \frac{1}{R^3}
\end{aligned}
\tag{14}
$$

Applying these simplifications to (13) gives the expression for the total head loss in the soil:

$$h_s = \frac{1}{R}\frac{A\,G\,Q_s}{4\pi} + \frac{1}{R^3}\frac{B\,G^2\,Q_s^2}{48\pi^2} \tag{15}$$

Orifice Losses

The standard orifice equation (1) is strictly only valid when the diameter of the orifice is at least 2 times the wall thickness. In other cases the coefficient of discharge needs to be modified to account for the extra frictional loss due to the length of the passage. If the flow through the orifice is assumed to be turbulent this loss can be associated with the standard turbulent pipe loss (Bear 1988). The total loss through the orifice is then given by:

$$h_o = \frac{8Q_o^2}{\pi^2 g d_o^4}\left(k + f\frac{t}{d_o}\right) \tag{16}$$

where f is the Hazen-Williams friction factor of the orifice, and t is the pipe wall thickness. It can be seen that as the ratio of the wall thickness to orifice diameter decreases the second term in the brackets in equation (16) becomes negligible and the standard equation for head loss through an orifice is recovered. It should be noted that it is assumed that k is independent of the orifice diameter. In the following work $k' = k + f\frac{t}{d_o}$.

Orifice and Soil Coupling

The two equations that describe the flow through the soil and the orifice need to be combined to generate an overall expression for intrusion flow rate. Substituting (15) and (16) into (3) gives:

$$\Delta h = +\frac{8k'}{\pi^2 d_o^4 g}Q_o^2 + \frac{1}{R}\frac{A\,G}{4\pi}Q_s + \frac{1}{R^3}\frac{B\,G^2}{48\pi^2}Q_s^2 \tag{17}$$

Obviously the total volumetric flow rate through the soil must equal that which enters the orifice, $Q_s = Q_o = Q$. Similarly the area of the internal boundary of the soil domain should equal that of the orifice.

$$\frac{\pi d_o^2}{4} = \frac{4\pi R}{G} \tag{18}$$

Rearranging for R gives:

$$R = \sqrt{G}\frac{d_o}{4} \tag{19}$$

Thus R is proportional to the size of the orifice, typically of the order of millimetres and given that pipe burial depths, D, are typically greater than 1 metre the assumptions made in Section 3 are valid.

The expression relating the intrusion flow rate and the head loss in the pipes is therefore given as:

$$\begin{aligned} \Delta h =& \frac{8k'}{\pi^2 d_o^4 g} Q^2 + \frac{\sqrt{G}\,A}{d_o \pi} Q + \frac{4}{3}\frac{\sqrt{G}\,B}{d_o^3 \pi^2} Q^2 \\ 0 =& \frac{8}{\pi^2 d_o^4 g}\left(k' + \frac{d_o g \sqrt{G}\,B}{6}\right) Q^2 + \frac{\sqrt{G}\,A}{d_o \pi} Q - \Delta h \end{aligned} \tag{20}$$

As equation (20) is a quadratic in Q an analytical solution for the steady-state intrusion flow-rate can be found:

$$Q = \frac{\pi d_o^2}{4}\left\{\frac{-d_o g\sqrt{G}A + g\sqrt{d_o^2 G A^2 + 32/g\left(k' + d_o g\sqrt{G}B/6\right)\Delta h}}{4\left(k' + d_o g\sqrt{G}B/6\right)}\right\} \tag{21}$$

It is worth investigating this equation further as a number of simplifications can be made under certain realistic conditions. Using the standard notation for quadratics where

$$a \cdot Q^2 + b \cdot Q + c = 0 \tag{22}$$

$$\begin{aligned} a =& \frac{8}{\pi^2 d_o^4 g}\left(k' + \frac{d_o g \sqrt{G}\,B}{6}\right) \\ b =& \frac{\sqrt{G}\,A}{d_o \pi} \\ c =& -\Delta h \end{aligned} \tag{23}$$

If the ratio $\frac{b^2}{-4ac}$ is greater than about 5 the square term in (22) is not significant and the flow-rate can be found by simply $Q = -\frac{c}{a}$:

$$Q = \frac{d_o \pi}{\sqrt{G} A} \Delta h \tag{24}$$

There are two possible cases where this situation will occur, the most likely is if c the driving pressure difference is small. In this case regardless of the properties of the porous media the flow velocities will be small, and as described in Section 3 the head loss in the soil will then follow Darcy's linear law. The second case is when the viscous resistance of the soil (A) significantly exceeds the Inertial resistance (B). If the porous properties for a granular media are calculated from the Ergun (6) then high Viscous resistances are seen for low porosity (highly packed) materials composed of particles with small mean grain diameters, typically very fine sands and silts.

If the ratio $\frac{b^2}{-4ac}$ is small, typically less than 10^{-3} then the linear terms of Q in (22) can be neglected and the flow-rate is found via $Q = \sqrt{-\frac{c}{b}}$. By substitution of (23) and some rearrangement the following formula is generated:

$$Q = \frac{1}{\sqrt{k' + \frac{d_o g \sqrt{G} B}{6}}} \frac{\pi d_o^2}{4} \sqrt{2g\Delta h} \tag{25}$$

It clear that this equation has a similar form to the standard orifice equation (1). The simple coefficient of discharge is however replaced by a function of the orifice diameter, the inertial resistance of the porous media, the frictional losses in the orifice and the geometric shape factor G. Further it can be seen that the expression simplifies exactly to the orifice equation by setting $B = 0$, the situation where there is no resistance from an external porous media.

Analytical Results

Figure 2 shows typical results generated from the newly derived intrusion expression, Equation (21). In Figure 2 the solid line shows the steady-state intrusion rate predicted for water only external to the pipe, the simple orifice equation. The other lines show decreasing flow rates due to increasing resistance of the external porous media. It can also be seen in Figure 2 that for a high value of the viscous resistance, A, the linear terms predominate over squared terms resulting in a flatter shape to the pressure / flow response. For the relatively large orifice size shown in Figure

2, the effects of the porous media are very apparent. For smaller diameter orifices the presence of the porous media has decreasing effect on the overall intrusion rate, this is due to the orifice losses predominating over the losses in the soil.

VERIFICATION AND VALIDATION OF THE INTRUSION MODEL

Two methods were used to provide verification of the intrusion volumes predicted by the model derived in this article. Firstly the model is compared to the results of the CFD model of a pipe, orifice and surrounding porous media described in Collins *et al.* (Collins et al. 2010). Secondly experimental results were obtained of the leakage and intrusion flow rates into a consolidated and constrained porous media, using an experimental facility at the University of Sheffield.

Verification Using CFD Modelling

A number of CFD models of the intrusion process for different orifice diameters were created using commercially available Fluent modelling software (ANSYS 2006), and used to assess the intrusion rates for different external porous resistances.

Figure 3 is a schematic of the modelled geometry. The meshed 3D model consists of the pipe volume, the surrounding porous media and the through wall thickness circular leak. Model geometries with a 10 mm diameter circular orifice located at the top of the pipe were assessed. The flow rate is calculated through a plane that runs through the leak orifice at the mid wall thickness.

The porous media surrounding the pipe is modelled as a fully saturated homogeneous isotropic porous continuum, implemented as a momentum source/sink term in the standard Navier-Stokes equations. The source term contains both a viscous and inertial resistance as in (5). In Collins *et al.* (2010) the coefficients of the viscous and inertial resistance were determined by the Ergun relationship as in (6). The input particle diameter, porosity and the output values of A and B are given in Table 1. Different values of the geometric shape factor were investigated, with the best fit being found when $G = \frac{1}{\sqrt[4]{d_o}}$, this value was then used through out.

Figure 4 shows steady-state results from the CFD model compared to the results obtained from the new analytical expression, Equation (21). In the figures the dashed lines are CFD results, the solid lines are the results from (21). It is clear that there is very good agreement between the two models. Figure 2 used a representative range of parameter values for the porous media, while Figure 4 uses values that are predicted by the Ergun equation. Comparison of the Figures shows the impact of a range of porous properties.

Experimental Validation

Experimental Set-up

To measure intrusion volumes through various porous media and orifice combinations an experimental intrusion element was built. This was composed of a large diameter outer pipe, capped at both ends, through which a small diameter pipe runs. Figure 5 shows a schematic of the intrusion element. The volume between the two pipes was filled with porous media, see Figure 6. The inner pipe was 50 mm internal diameter Medium Density Polyethylene (MDPE) pipe with 6 mm wall thickness, this pipe was capped at both ends, one cap being fitted with an inverse U-bend. The external pipe consists of a 380 mm diameter, 8 mm wall thickness Acrylonitrile Butadiene Styrene (ABS) pipe. CFD simulations after Collins *et al.* (Collins et al. 2010) were undertaken to determine that the external pipe was of sufficient size such that the flow field through the porous media was not significantly affected by the boundary of the external pipe, for the ranges of pressures and flows used in these tests. The external pipe is 400 mm in length and has 12 1/4“ British Standard Pipe (BSP) tappings equally spaced (in three groups of four around the circumference) to allow for the water egress, see Figure 5. A final tapping point on the top of the pipe at the mid-length point was added to allow for air removal and as a pressure measurement point, using a Gems Sensors 2200.

The steady state intrusion process was driven by an external pressure applied to the tapping points of the outer pipe. An internal pipe pressure of 70 mm was maintained by the inverse U-bend, ensuring the internal pipe was kept full at all times. Intrusion flow rates were measured at the outlet of the U-bend, using a time/volumetric method. Due to the low flow rates in the porous media the static pressure at the leak was assumed to be the height difference between the sensor and the leak position. A range of orifice sizes and porous media combinations were then testes by varying the external pressure and measuring the corresponding flow rate.

In preliminary tests it was found that there was a large amount of variability in results due to inconsistencies in packing the porous media into the intrusion element. In addition there was evidence of movement of the particles during the tests. To overcome this a bladder was installed in one end of intrusion element which when filled with water and pressurised, prevented the movement of the particles and ensured a consistently compacted and consolidated porous media.

Experimental Method

To run an intrusion test an inner pipe with the required leak orifice was installed. The selected porous media was then carefully packed around the pipe and compacted, whilst the intrusion element was in the vertical position. When the required level of fill was achieved the bladder was placed on top of the gravel and the end cap firmly attached and sealed. The bladder was then inflated and the whole intrusion element was rotated to the horizontal position (see Figure 6) with the leak orifice on the top of the pipe. Once in this position the intrusion element was filled with water to saturate the porous media, carefully bleeding air through the tapping a the highest point on the external pipe. A test run comprised of pressurising the external head measuring the intrusion flow rate three times and then sequentially raising the external head across the required range. Once the highest required pressure had been reached the pressure was returned to the lowest value and the flow measured again to ensure the tests had not altered the porous media properties during the test. The range of driving pressures used was 0 - 9 m in 1 m increments. In reality the driving force would generated by low pressures in the pipeline limited to the cavitation pressure at around -10 m. For each orifice and media combinations tested three repeat tests were conducted. Between tests the porous media was disturbed and re-packed following the same procedure.

Orifice Size and Porous Media

It was decided to test only round orifices to negate any variability due to pressure dependent area changes associated with cracks. Orifices were drilled with diameters of 1, 2 and 10 mm. It was noted that due to visco-elastic effects the actual orifice size achieved was different to that drilled. The actual size of each orifice was measured 4 times with digital callipers, the average value is given in Table 2. To determine the coefficients of discharge of the orifices, tests were carried out with no porous media present. The coefficients were then found by fitting the results to the standard orifice equation, Table 2.

Three different porous media, in addition to water only, were investigated in this study: 6 mm smooth spherical plastic balls (BB's); 6.25 - 9.5 mm Pea Gravel (Gravel 1); 3.25 - 5.5 mm Pea Gravel (Gravel 2). Spherical beads were included to provide a consistent homogeneous porous media without the inherent variability of graded gravel. The two gravels were chosen to represent the British standard for pipe burial of 5 - 10 mm pea gravel (BS-CP312-1 1973).

The resistance to flow generated by the porous media is one of two primary input variables for the new model, the other being the orifice loss coefficient. Literature reports a range of viscous and inertial resistance coefficients dependent on the porous media in question, and that these can be significantly different to those generated from the Ergun equation. Therefore experiments were conducted to accurately measure the resistances effects of the different porous media used. An 800 mm long section of the inner test pipe was packed with media, capped with mesh screens at each end, and then pressurised at one end to a range of values with the resulting flow rate and pressure drop being measured. Tests were repeated 3 times for each porous media with the pipe section repacked between each. In order to account for the effects of the mesh screens results from water only tests were then subtracted and a parabolic regression fit undertaken to determine the porous resistance properties of each media. The results and parametric values including the regression coefficients are given in Figure 7 and Table 3. The smooth regular BBs gave consistent results, with low resistance compared to the gravel.

The resulting parametric values, particularly those of the gravels, are found to be significantly different, with a higher A and lower B coefficient, to those predicted by the Ergun equation that had previously been used for the CFD modelling.

Validation Results

Figures 8 to 10 show the steady-state results from experiments with the three different orifice sizes and three different porous media, and water only, for the range of driving pressures. Results from the analytical expression are included as lines, calculated using the properties of the orifice and porous media given in Tables 2 and 3. Computation CFD results are not included as they have previously been shown to be virtually indistinguishable from the analytical outputs. Unfortunately the control of the driving head during the tests was poor, oscillated around the required value, accounting for some of the scatter in the data that is visible in Figures 8 to 10.

Figure 8 shows the result for the 1 mm drilled orifice. It can easily be seen that the results for experimental tests with porous media present are indistinguishable from those with water only. Hence for orifices with small diameters, particularly in relation to the wall thickness, it appears that the orifice losses dominate those of the porous media. Therefore the experimental relationship between intrusion flow and pressure collapses to the standard orifice equation, (1). The analytical results from the new expression correctly predict that the media effects are insignificant, showing negligible difference between the cases when a porous media is present or not.

Figure 9 shows the results for the 2 mm drilled orifice. Due to the scatter in the data, and small differences due to the porous media effects it is hard to draw clear conclusions on the impacts of the porous media from the experimental results by eye. However if curves are fitted to the data (not shown) it is possible to discern that gravel 1 and 2 are not equal to the water only case, with Gravel 2 having a greater effect than gravel 1. There is little or no distinction between the BBs and water only results. The analytical expression developed in this article predicts small effects due to the porous media, generally predicting slightly greater impacts than the measured data. The trend for greater impact from gravel 2 than 1 is correctly predicted. Overall it is apparent that, as with the 1 mm drilled case, the effects of the 2 mm drilled orifice still dominate over those of the porous media, for both the experimental data and analytical outputs.

Figure 10 shows the results for the 10 mm drilled orifice. In this case the resistance of the porous media has an appreciable effect on the resultant intrusion flow rates. The experimental data shows clear distinction between the different porous media. The BBs with the smallest resistances have the smallest effect as expected, with Gravel 2 the largest. In absolute terms the impact of porous media can be seen to be increasing with negative driving head. The outputs of the analytical expression generally show reasonable agreement with the experimental data, tending to provide a lower bound (as was the case for Figure 9) and with improving quality of fit with increasing driving head.

DISCUSSION

The new results presented in this paper, from the derived analytical expression and the validating experimental results, show that the existence of a porous media external to a pipe orifice will affect the intrusion flow rates for a given steady-state pressure. Both the experimental and the analytical results show that the effect of the porous media is more pronounced for larger orifice sizes and that both the resistance and inertia properties of the media are important. For very small orifices, the orifice losses appear to be the dominating effect, collapsing back to the response predicted by the standard orifice equation, with appropriate fitted C_d value). From Table 2 it can be seen that the fitted (to the water only experimental data) coefficient of discharge for the 1 mm orifice is significantly smaller than for the other size orifices. This can be accounted for by significant piping loses being present in addition to the inlet and outlet losses, see Section 3. Therefore for small diameter holes and cracks of narrow diameter, relative to the pipe wall thickness, where piping losses will be a significant factor, one should use lower C_d values. This is consistent with the theory of the the flow through cracks and orifices expounded in, for instance, Massey (1998).

The derivation of the analytical expression in Section 3 makes a number of simplifications and assumptions that it is important to re-consider. Firstly, it is assumed that the pipe is buried a significantly depth in a saturated porous media. This allow the external boundary of the integration domain to be large, allowing the assumption that the flow rate at the boundary is negligible, and is therefore in effect a free surface. The saturated condition also allows any movement of the free surface to be ignored, realistic if the saturated region is sufficiently large. A further extension to this work could consider the effects of intrusion from unsaturated porous media. It is debatable whether the resultant differences would be significant. A pre-requisite for intrusion is a leakage point, and it is likely that the water leaking out of this orifice, under normally high operating pressures, would create a large region around the pipe that is close to being saturated. These saturated conditions were certainly valid for the experimental set up used. Secondly it is assumed that the flow into the orifice is driven by a steady pressure and is completely radial, that the deflection of the flow paths around the pipe are negligible. Results from CFD simulations for flows into an orifice presented in Collins *et al.* (2010) show that flows can enter from all directions around the pipe, and that the zone of influence of pressure effects around the pipe is approximately spherical but that there is a local distortion due to the pipe. The close agreement of the analytical and CFD outputs suggest that this assumption is valid. Thirdly, the porous media has been assumed to be a perfectly homogeneous and isotropic continuum. By making this assumption we are applying average effects of the resistance to the flow that a large number of particles would have and applying that to the entire integration regime. Given that it is impossible to know the exact orientation of particles in the porous media, and even if it was possible, the calculations required to generate resistances would be prohibitive, this seems reasonable. Very close to the orifice, where the flow may pass only 1 or 2 particles of porous media the continuum assumptions may break down. An additional area where the continuum assumptions may break down is the wall effects of the pipe. Due to the presence of the solid surface of the pipe, the packing of the porous media is not as dense as in the rest of the continuum (Taylor et al. 2000), potentially providing a preferential pathway for flow along, and/or around, the pipe. This condition is not considered in the analytical expression due to the simplification described above that the flow is perfectly radial. Nor is this condition described by the CFD calculations where the continuum model is allowed to extend perfectly to the wall of the pipe. This preferential flow path could explain the slightly greater intrusion flow rates measured in the experiments, compared to the lower bound solution provided by both the analytical and CFD results.

The experimental results were obtained from a specially designed intrusion element. CFD models were generated for the design of the element so that the sphere of influence in the porous media was well within the boundary of the outer pipe section. The 12 tapping points used to apply the driving head where also modelled to ensure that they did not have a significant effect on the resultant flow field in the porous media. Hence there is good confidence in the experimental configuration used. However the driving head was applied from the mains supply in the laboratory and was found to be significantly variable between the tests. This resulted in a scatter in the experimental data. If the tests were to be repeated, care should be taken that the pressure source is carefully isolated and well controlled.

In addition to orifice size and coefficient of discharge required by the orifice equation, the new analytical expressions requires inputs for the properties of the porous media. In real networks, when trying to assess the risk of intrusion, the size, shape and location of orifices will always be uncertain. The additional requirements to describe the porous media properties of the surrounding ground conditions add to this uncertainty. However, it can be seen from the comparison of the experimental and analytical results that the new expression tends to predict a lower bound of the measured flow rates, while an absolute upper bound to measured intrusion flow rate is provided by the water only standard orifice equation. By selecting realistic, if not perfectly precise, porous properties the new expression and the standard orifice equation can be effectively used to provide upper and lower bounds on the potential intrusion respectively. While this does not perfect represents the actual situation, it provides a significant increase to understanding the potential risk associated with intrusion events.

Leakage

Although developed to try and describe intrusion processes, the analytical expression derived is theoretically reversible and thus able to estimate leakage flow rates. In order to validate the applicability of the expression for leakage calculations a further set of experiments were conducted. For these tests the intrusion element described above was installed in a pipe test facility at the University of Sheffield, with the inner pipe becoming part of a 150 m long pipe loop of the same material. A wide variety of flows (up to 2 m/s or 0.004 m3/s) and pressures (up to 45 m) can be generated in the pipeline, although in for these tests the flow loop was statically pressurised up to 30 m. For this exploratory test the same 10 mm orifice, which showed greatest variation for intrusion, was used now as a leakage point. The 12 tapping points on the outer pipe where connected together using increasing diameter pipe lengths and through an inverted U-bend, to ensure that the media remained fully saturated at all times. Leakage flow rates were measured at the outlet of the U-bend, using a time/volumetric method.

In a paper by Clayton and van Zyl (2007) it was hypothesised that the dynamics of media (soil movement, fracture and fluidisation) surrounding a leakage aperture may have a significant effect on the leakage flow rate. These effects are currently not well understood with respect to leaks. To provide an idealised validation situation for the analytical expression, which does not model dynamic porous media effects, the porous media was again fully consolidated and constrained to prevent fluidisation and to provide homogeneous and isotropic steady conditions. This was maintained during tests by the application of the steady pressure to the compression bladder in excess of the leakage pressure, as in the intrusion experiments.

Figure 11 shows comparison of the experimental leakage rates for 10 mm drilled orifice in the same range of media considered for intrusion case. It can be seen that similarly to the intrusion case, the analytical expression exhibits the same shape curve as the leakage experiments. Similar to the intrusion case the analytical expression slightly under predicts the leakage rate. Again it is hypothesised that this is due to the preferential paths around the leak, and potential movement in the soil despite the compacting pressure. In the leakage case a higher range of pressures were available, and the relationship with the analytical expression appears to be maintained up to the high pressures. A better level of control of was achieved in the driving pressures, as a results a decreased level of scatter can be seen in the data. From the results, it appears that the analytical expression provides a good fit to the data when the assumptions of static and homogeneous external media can be made.

CONCLUSIONS

A new analytical expression to describe flow into pipes, with an aperture, buried in porous media (intrusion) is presented and validated in this paper. The expression improves on the orifice equation by considering viscous and inertial effects of the surrounding media and accounts for external 3D effects by making the assumption of an idealised point sink for the aperture. The analytical expression has been verified against a full 3D CFD model of the intrusion process, and good agreement found. To fully validate the analytical expression, a series of experiments that allow true 3D flow in an external porous media were carried out. These experiments provide quantification of intrusion flow rates for a range of driving pressures and different porous media.

The analytical expression was found to give a close match to the experimental results, generally giving a lower bound to the intrusion flows. The analytical expression is conceptually reversible for application to leakage, and experiments were conducted to validate this. Good agreement was again found when assumptions of static hydraulic conditions and fully compacted and consolidated porous media could be made. As with the intrusion case, the analytical expression tended to slightly under estimate the amount of leakage. The lower bound nature of the new expression, in comparison to physical results, may be due to preferential flow paths at the pipe media interface. There is potential for further work to investigate dynamic effects on the intrusion and leakage process, whether that be due to the changing external media properties or due to dynamic changes of pressure as a driving force.

The experimental, analytical and CFD results presented here have shown that the coupled porous media and orifice effects cannot be ignored when considering either intrusion or leakage associated with buried pipelines. Future realistic modelling, such as to assess the potential health risk due to intrusion events, should therefore include these. The new expression can be used, in combination with the standard orifice equation, to provide previously unavailable upper and lower bound limits for intrusion and leakage flow rates.

Acknowledgements This work was supported by the EPSRC grant EP/G015546/1, the "Contaminant Ingress into Distribution systems (CID)" project.

REFERENCES

ANSYS (2006). "Ansys Fluent Release 6.3 User Guide." *Report no.*, Ansys Inc.

Barr, D. (2001). "Turbulent flow through porous media." *Ground Water*, 39(5), 646–650.

Bear, J. (1988). "Dynamics of flow in porous media." *New York: Dover*.

Besner, M., Ebacher, G., Lavoie, J., and Prévost, M. (2007). "Low and Negative Pressures in Distribution Systems: Do They Actually Result in Intrusion?." *Proceedings of the World Environmental Resources Congress*, ASCE.

Boyd, G., Wang, H., Britton, M., Wood, D., Funk, J., and Friedman, M. (2004a). "Intrusion within a simulated water distribution system due to hydraulic transients. I: Description of test rig and chemical tracer method." *Journal of Environmental Engineering*, 130, 774.

Boyd, G., Wang, H., Britton, M., Wood, D., Funk, J., and Friedman, M. (2004b). "Intrusion within a simulated water distribution system due to hydraulic transients. II: Volumetric method and comparison of results." *Journal of Environmental Engineering*, 130, 778.

BS-CP312-1 (1973). "Code of practice for plastics pipework (thermoplastics material). General principles and choice of material." *Report no.*, British Standards Institute.

Cassa, A. and Van Zyl, J. (2011). "Predicting the head-area slopes and leakage exponents of cracks in pipes." *Proceedings of CCWI 2011*.

Collins, R., Beck, S., and Boxall, J. (2011). "Intrusion into water distribution systems through leaks and orifices: Initial experimental results." *11th Computing and Control in the Water Industry 2011*.

Collins, R., Besner, M., Beck, S., Karney, B., and Boxall, J. (2010). "Intrusion Modelling and the Effect of Ground Water Conditions." *Proceedings of Water Distribution System Analysis*.

Ergun, S. (1952). "Fluid flow through packed columns." *Chemical Engineering Progress*, 48, 89–94.

Fleming, K., Dugandzik, J., and LeChevallier, M. (2007). *Susceptibility of Distribution Systems to Negative Pressure Transients*. American Water Works Association.

Forchheimer, P. (1901). "Wasserbewegung durch boden." *Z. Ver. Deutsch. Ing*, 45, 1782–1788.

Friedman, M., Radder, L., Harrison, S., Howie, D., Britton, M., Boyd, G., Wang, H., Gullick, R., LeChevallier, M., Wood, D., et al. (2004). *Verification and control of pressure transients and intrusion in distribution systems*. AWWA Research Foundation and US Environmental Protection Agency.

Gullick, R., LeChevallier, M., Svindland, R., and Friedman, M. (2004). "Occurrence of transient low and negative pressures in distribution systems." *Journal American Water Works Association*, 96(11), 52–66.

Karim, M., Abbaszadegan, M., and LeChevallier, M. (2003). "Potential for pathogen intrusion during pressure transients." *Journal- American Water Works Association*, 95(5), 134–146.

Kirmeyer, G., Friedman, M., and Martel, K. (2001). *Pathogen intrusion into the distribution system*. American Water Works Association, Denver.

LeChevallier, M., Gullick, R., Karim, M., Friedman, M., and Funk, J. (2003). "The potential for health risks from intrusion of contaminants into the distribution system from pressure transients." *Journal of Water and Health*, 1(1), 3–14.

Lindley, T. and Buchberger, S. (2002). "Assessing intrusion susceptibility in distribution systems." *Journal- American Water Works Association*, 94(6), 66–79.

Lopez-Jimenez, P., Mora-Rodriguez, J., Carcia-Mares, F., and Fuertes-Miquel, V. (2010). "3D computational model of external intrusion in a pipe across defects." *Proceedings of the 2010 International Congress on Environmental Modelling and Software*, International Environmental Modelling and Software Society.

Massey, B. (1998). *Mechanics of Fluids*. Taylor & Francis.

Taylor, K., Smith, A., Ross, S., and Smith, M. (2000). "CFD modelling of pressure drop and flow distribution in packed bed filters." *PHOENICS Journal of Computational Fluid Dynamics and its applications*, 13(4), 399–413.

Van Zyl, J. and Clayton, C. (2007). "The effect of pressure on leakage in water distribution systems." *Water management*, 160(2), 109–114.

Walski, T., Bezts, W., Posluszny, E., Weir, M., and Whitman, B. (2006). "Modeling leakage reduction: through pressure control." *Journal- American Water Works Association*, 98(4), 147–155.

Walski, T. and Lutes, T. (1994). "Hydraulic transients cause low-pressure problems." *Journal American Water Works Association*, 86(12), 24–32.

List of Tables

TABLE 1. Table of porous media properties from Collins *et al.* (2011)

Case	Condition	D_p (m)	ϵ (-)	A (s m^{-1})	B (s^2 m^{-2})
1	Free Fluid	-	-	-	-
2	Loose Gravel	0.01	0.4	0.8633	167.24
3	Compact Gravel	0.01	0.25	5.5255	856.27
4	Loose Sand	0.001	0.4	86.337	1672.40
5	Compact Sand	0.001	0.25	552.554	8562.69

TABLE 2. Table of the measured orifice and best fit coefficient of discharge

Orifice	Average Measured Diameter	C_d
1 mm	0.4 mm	0.45
2 mm	1.55 mm	0.59
10 mm	9.6 mm	0.57

TABLE 3. Table of average porous properties of the 3 different media used in the study and the values of the regression fit.

Media	A	B	R^2
BB's	9.88	102	0.999
Gravel 1	13.7	188	0.994
Gravel 2	19.4	252	0.991

List of Figures

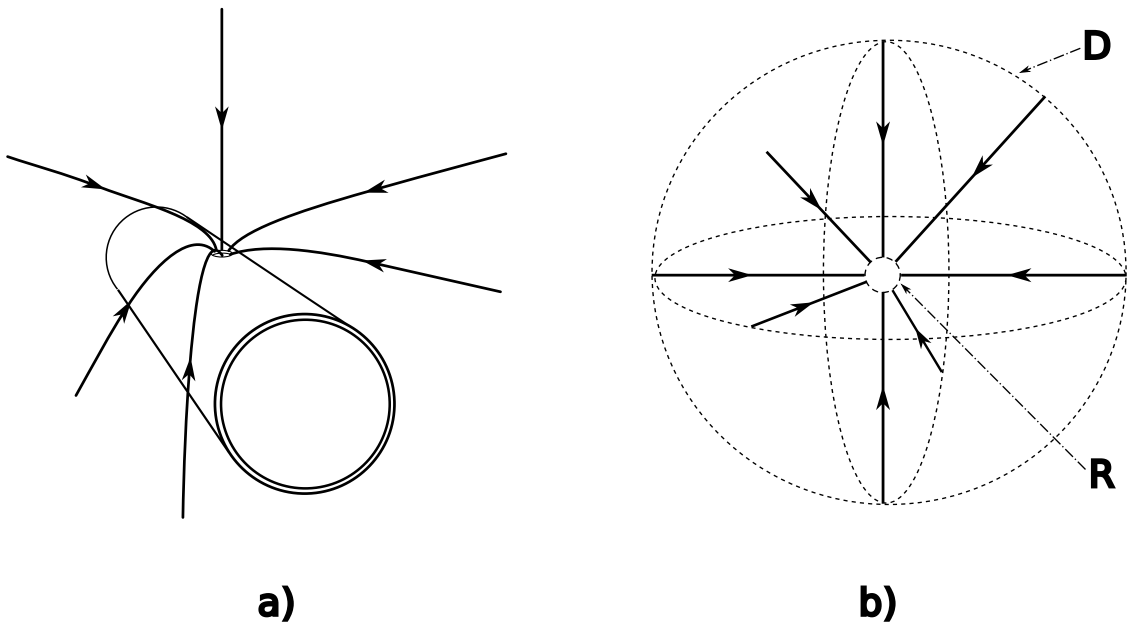

FIG. 1. Flow into a submerged orifice, a) actual case, b) conceptual model, showing D the external boundary of the model, and R the internal boundary

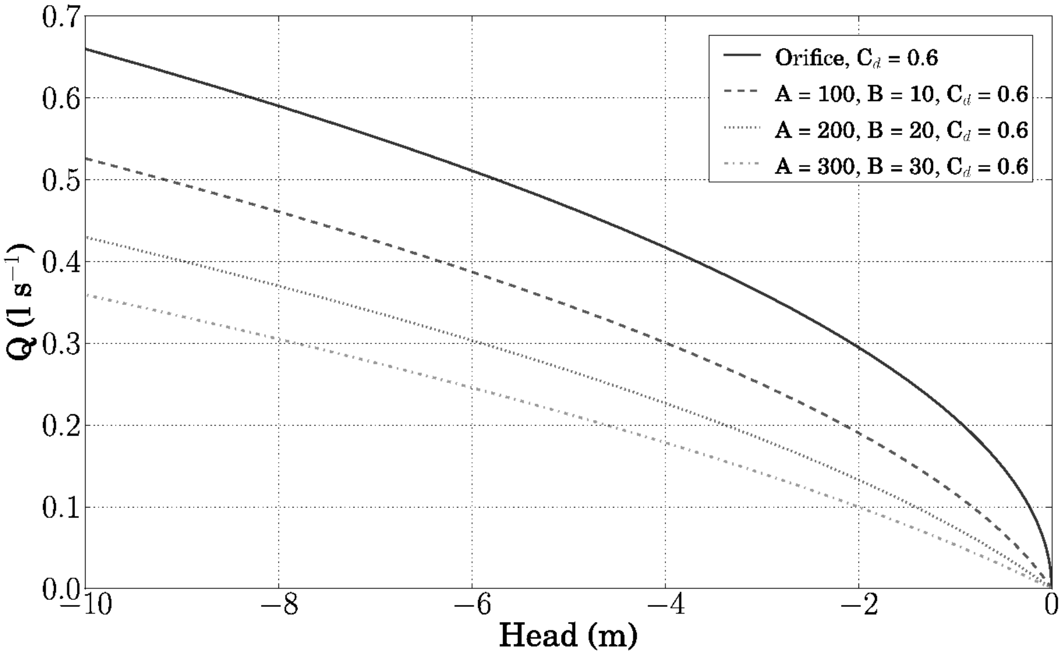

FIG. 2. Typical output of the new steady state analytical intrusion model showing the effect of different porosities and orifice losses for a 10 mm circular orifice

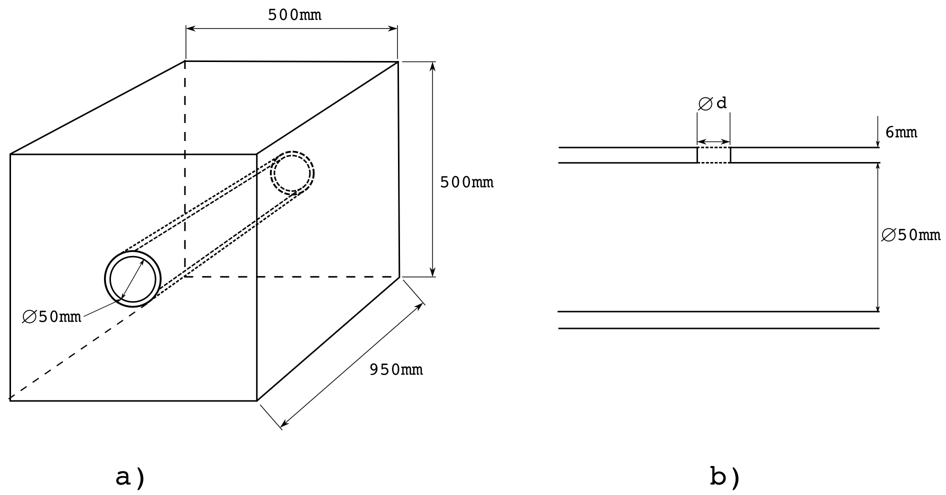

FIG. 3. Schematic of the modelled geometry, a) shows the pipe and the boundary of the porous media, b) is a cross section of the pipe showing the location of the leak orifice. Data from Collins *et al.* (2010)

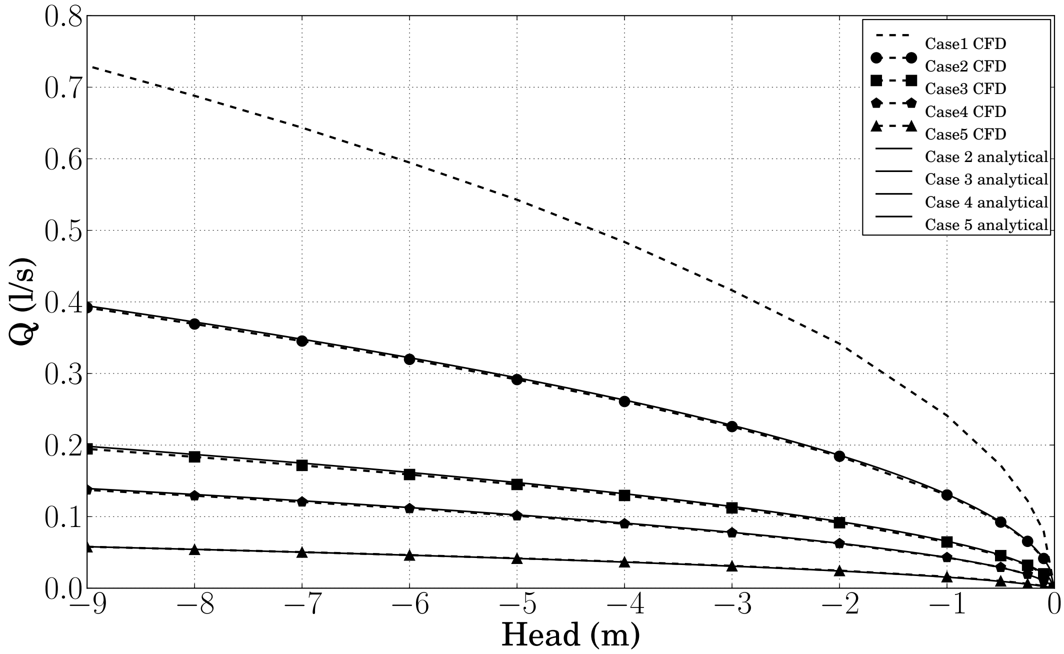

FIG. 4. Comparison of the results for intrusion volumetric flow rates predicted by the CFD simulation and the newly derived analytical expression for different media cases, see Table 1, for a 10 mm circular orifice. Dashed lines are CFD results, solid lines the newly derived analytical expression

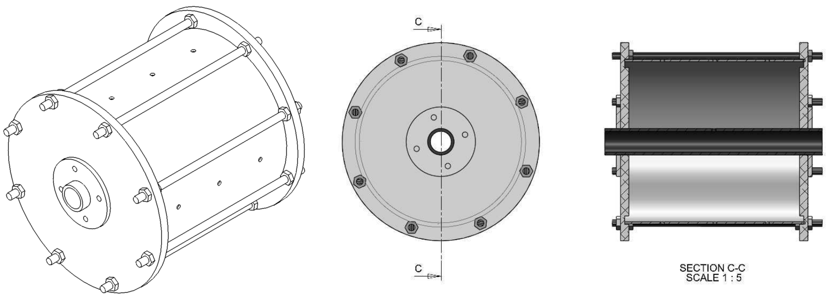

FIG. 5. Schematic of the experimental intrusion element

a) 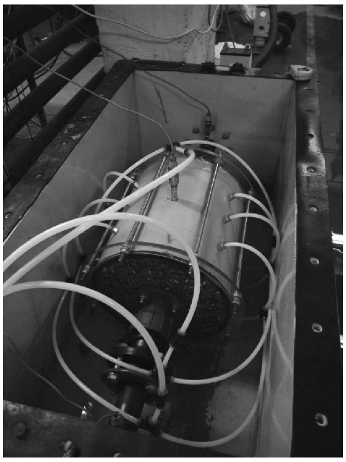 b) 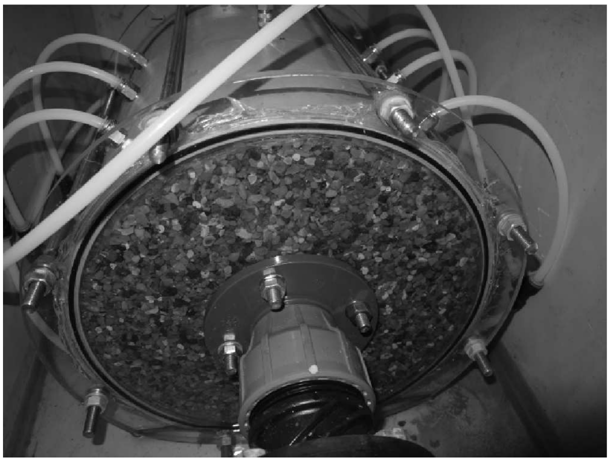

FIG. 6. Experimental intrusion element a) showing the external pipe and the 12 pipes used to feed water into the porous media. b) Close up of the porous media compacted in the intrusion element

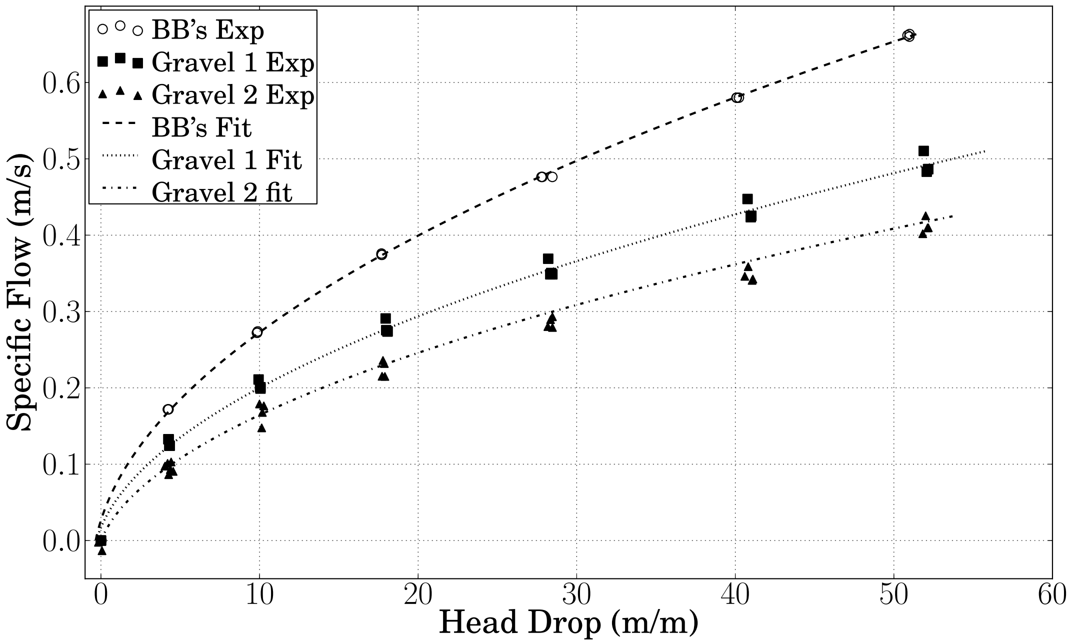

FIG. 7. Determination of the porous properties of the BB's and the two Gravel Media used in the test. Experimental results are given by the points, the solid lines are fitted 2nd order polynomials.

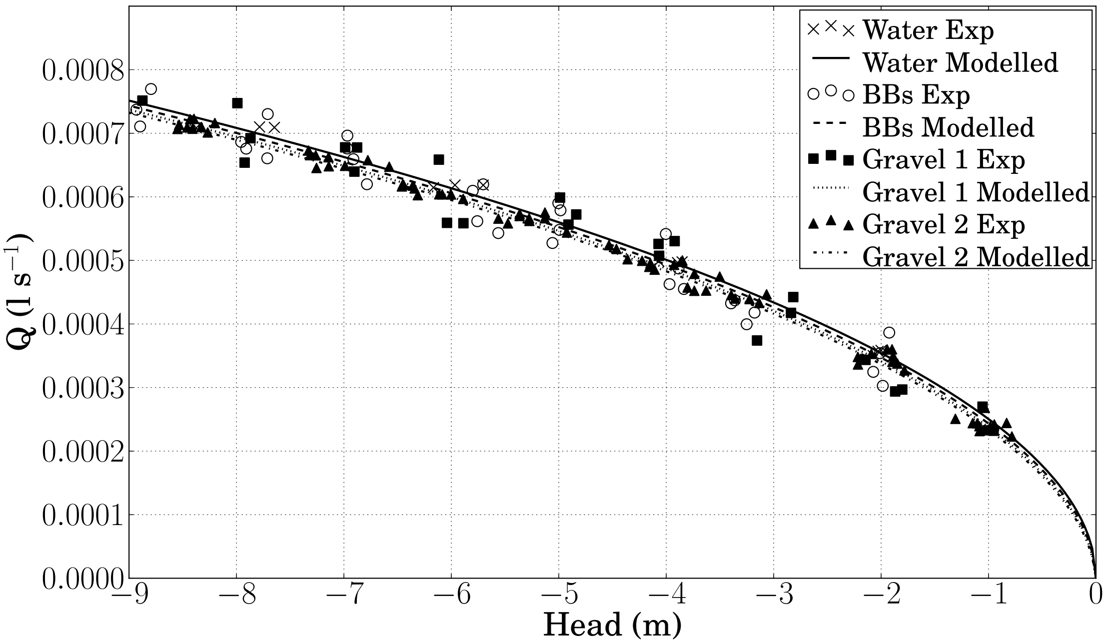

FIG. 8. Comparison of the experimental results and the outputs of the analytical expression for intrusion into a 1 mm orifice. Experimental results are given by the points, the analytical expression with the lines

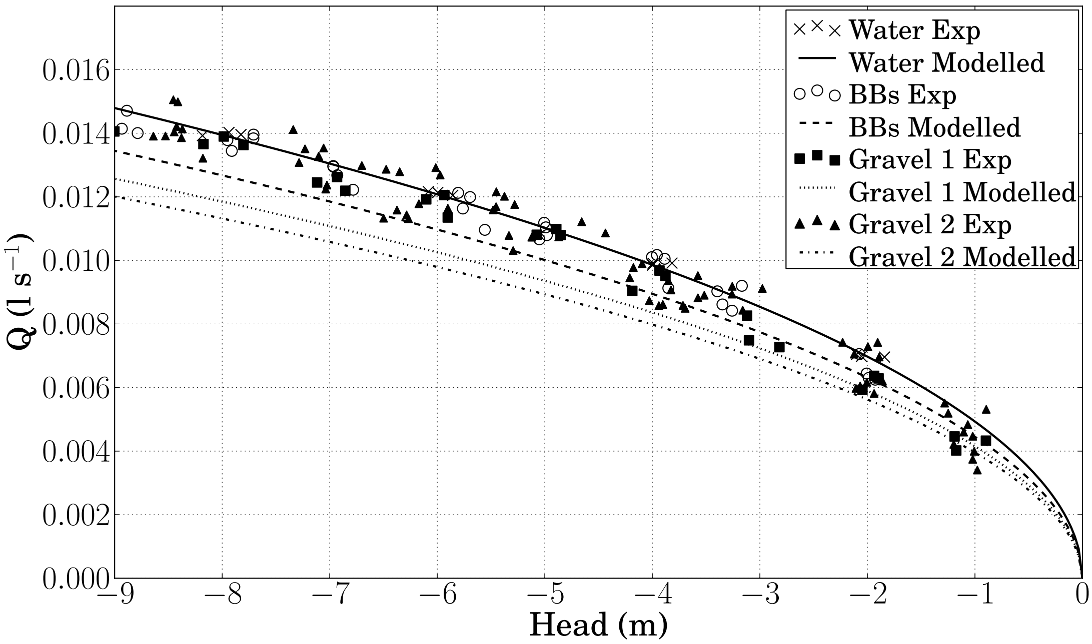

FIG. 9. Comparison of the experimental results and the outputs of the analytical expression for intrusion into a 2 mm orifice. Experimental results are given by the points, the analytical expression with the lines

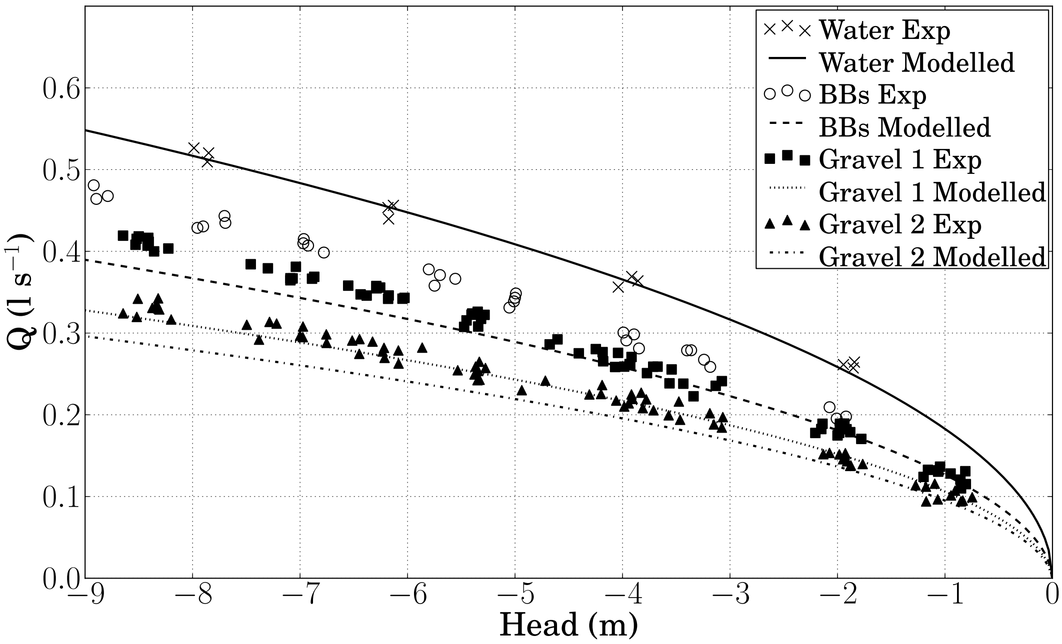

FIG. 10. Comparison of the experimental results and the outputs of the analytical expression for intrusion into a 10 mm orifice. Experimental results are given by the points, the analytical expression with the lines

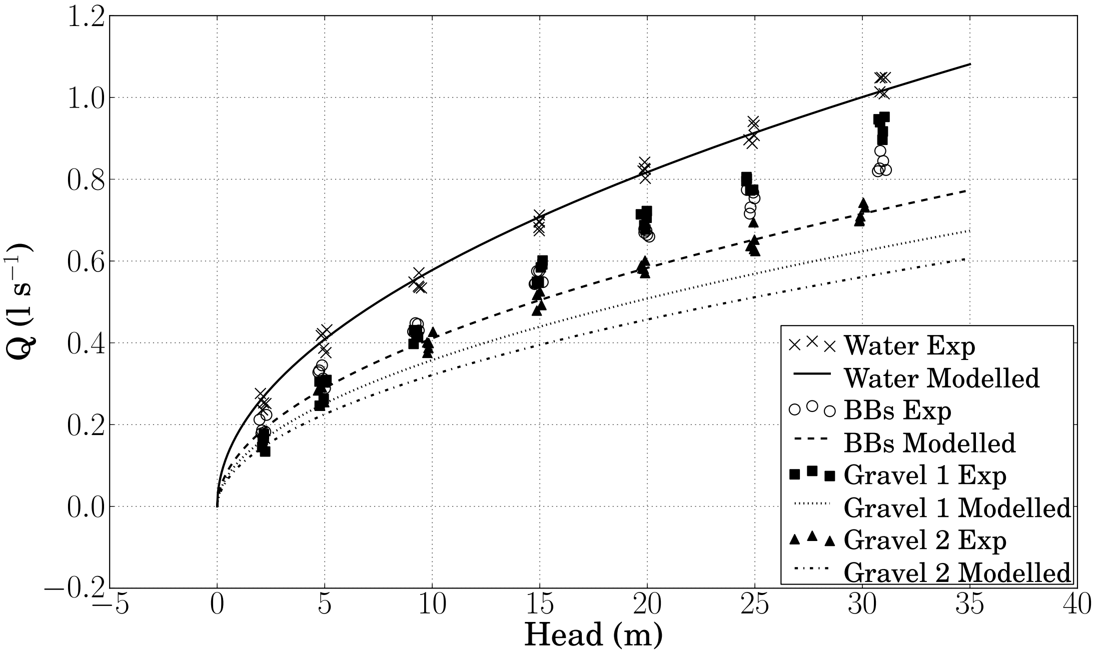

FIG. 11. Comparison of the experimental results and the output of the analytical expression for leakages out of a 10 mm orifice. Experimental results are given by the points, the analytical expression with the lines